Giant Electropleochroism in GaAs-(Al,Ga) As Heterostructures: The Quantum-Well Pockels Effect

S. H. Kwok,[1] H. T. Grahn,[2] K. Ploog,[2],[a] and R. Merlin[1]

[1]The Harrison M. Randall Laboratory of Physics, The University of Michigan, Ann Arbor, Michigan 48109-1120

[2]Max-Planck-Institut für Festkörperforschung, Heisenbergstrasse 1, W-7000 Stuttgart 80, Federal Republic of Germany

(Received 2 April 1992)

We report on the biaxial response of photoluminescence to electric fields in GaAs quantum-well structures. For fields along [001], emission due to nominally forbidden excitons exhibits substantial differences between [110] and [1$\bar{1}$0] polarizations. Transitions which are allowed within the envelope-function formalism show no noticeable anisotropy. In terms of symmetry, our observations relate to the linear electro-optic (Pockels) effect. The field dependence of the anisotropy is unusual in that it decreases with increasing field. Results can be qualitatively accounted for by perturbative analyses.

PACS numbers: 78.20.Jq, 73.20.Dx, 73.40.Kp, 78.55.Cr

Electric fields normal to the layers modify the optical properties of semiconductor quantum-well (QW) structures and superlattices in ways which depart appreciably from those affecting bulk materials [1-10]. This refers in particular to the quantum-confined Stark effect [1-4] and features such as Wannier-Stark localization and ladders [6-9] bearing on the problem of Bloch oscillations [10]. In this Letter, we report on a novel phenomenon relying on quantum confinement which relates to Pockels linear electrorefraction. Unlike previously considered phenomena where the optical uniaxial symmetry of the QW is maintained [1-9], the new effect manifests itself in a giant field-induced *biaxial* anisotropy (electropleochroism). A further associated distinction is that the relevant dependence on the field is *odd*, as opposed to even [11]. Enhanced Pockels-like anisotropy is observed in photoluminescence (PL), primarily from excitons such as e_2h_1 showing weak coupling to photons at zero field [12] (e_ih_j denotes states with one electron and one heavy hole in the ith and jth subbands, respectively). Consistent with recent near-gap measurements of linear electro-optic coefficients in GaAs-$Al_xGa_{1-x}As$ QW structures [13], we find no enhancement at the dominant e_1h_1 PL.

In zinc-blende (point group T_d) semiconductors, the presence of [001] electric fields leads to biaxial behavior [14] where the anisotropy in the plane perpendicular to the field distinguishes [110] from [1$\bar{1}$0]. Important as it is for some applications, however, this (Pockels) effect remains very small [15] up to the breakdown field ($<10^6$ V cm^{-1}). Below the band gap, the field derivative of the refractive index n at $F=0$ is given by $\partial n/\partial F \propto n^3 r_{41}$. Here, F is the z component of the field and r_{41} is the electro-optic Pockels coefficient. Experiments on bulk GaAs in the vicinity of the fundamental E_0 gap give $r_{41}\sim 1.5\times 10^{-10}$ V^{-1}cm, i.e., $(\partial n/\partial F)_{F=0}\sim 10^{-8}$ V^{-1} cm, with no significant wavelength dependence [16]. The corresponding value for the imaginary part of the index k is not well known. An estimate using optical-susceptibility $\chi_{14}^{(2)}$ data at the E_0 resonance [17] gives $|\partial k/\partial F|_{F=0}<10^{-9}$ V^{-1}cm. It will become evident later that these values are too small to account for our QW findings.

To discuss the mechanism for enhanced biaxial anisotropy, it is appropriate to focus first on the symmetry arguments underlying the problem. Let $\mathbf{F}$ be the static electric field and $\Psi(\mathbf{F})$ an excited state of the GaAs QW—say, an exciton of energy $\Omega(\mathbf{F})$—which couples to light. For photons polarized in the direction of the unit vector $\hat{\epsilon}$, we expand the intensity $\mathcal{I}$ emitted (or absorbed) at Ω as

$$\mathcal{I}=\sum_{kl}A_{kl}^{(0)}\epsilon_k\epsilon_l+\sum_{kl,m}A_{klm}^{(1)}\epsilon_k\epsilon_l F_m + \sum_{kl,mn}A_{klmn}^{(2)}\epsilon_k\epsilon_l F_m F_n+\cdots . \quad (1)$$

Here, the tensors multiplying $\mathbf{F}$ and $\hat{\epsilon}$ are invariant under operations of the QW D_{2d} group. In particular, the allowed form for $F_z=F$ and $F_x=F_y=0$ is

$$\mathcal{I}(\hat{\epsilon},F)=(\epsilon_x^2+\epsilon_y^2)I_{\parallel}^{+}(F)+2\epsilon_x\epsilon_y I_{\parallel}^{-}(F)+\epsilon_z^2 I_{\perp}^{+}(F) , \quad (2)$$

where I^+ and I^- ($|I_{\parallel}^-|\le I_{\parallel}^+$ and $0\le I_{\perp}^+$) are, respectively, the even and odd parts of $\mathcal{I}$ associated with the directions perpendicular ($\perp$) and parallel ($\parallel$) to the layers. As for bulk GaAs, the principal axes are [110], [1$\bar{1}$0], and [001]. Obviously, QW structures are already uniaxial ($I_{\parallel}^+\neq I_{\perp}^+$) at $\mathbf{F}=0$. Pockels-related effects require $I_{\parallel}^-\neq 0$ and follow from the absence of inversion symmetry. In the experiments, we determine the polarization ratio

$$\rho\equiv\frac{\mathcal{I}_{[110]}-\mathcal{I}_{[1\bar{1}0]}}{\mathcal{I}_{[110]}+\mathcal{I}_{[1\bar{1}0]}}=\frac{I_{\parallel}^-}{I_{\parallel}^+} \quad (3)$$

measuring the degree of in-plane anisotropy. The corresponding ratio for [100] and [010] is, of course, equal to zero.

A qualitative understanding of what determines the magnitude of ρ can be gained from first-order perturbation theory. As we shall see, the analysis discriminates between excitons e_ih_j with $i=j$ (electric-dipole allowed in the envelope-function approximation) and $i\neq j$ (forbid-

© 1992 The American Physical Society

den). Only the latter may exhibit enhanced anisotropy. To calculate the leading linear term of $\rho(F)$ or, alternatively, $(d\rho/dF)_{F=0}$, it is important to recognize that $I_{\parallel}^{-}$ is largely defined by field-mediated coupling of Bloch states as opposed to envelope functions. There are two basic contributions to $I_{\parallel}^{-}$ [18]: (i) a purely electronic one which involves coupling between E_0 states and higher-lying $\Gamma_{7,8}^{c}$ states of the conduction band [19] and (ii) a lattice term due to field-induced sublattice displacement [18] leading to heavy-light hole mixing. The corresponding hybridization parameters are (i) eFa_0/Δ and (ii) $\mathcal{D}d_{14}F/\delta$. Constants $\Delta \approx 3$–4.5 eV [19], $\mathcal{D} \approx 6$ eV, and $d_{14} = -2.7\times10^{-10}$ $\mathrm{V^{-1}cm}$ [20] represent, respectively, the separation between the $\Gamma_{7,8}^{c}$ states and the lowest conduction (Γ_6^c) and the top valence ($\Gamma_{7,8}^{v}$) band states at Γ, the [111] deformation potential, and the piezoelectric coefficient of GaAs; a_0 is the (hydrogen) Bohr radius and δ is a measure of the heavy-light hole splitting. Clearly, $eFa_0/\Delta \sim \mathcal{D}d_{14}F/\delta \ll 1$ for typical well thicknesses and fields.

For allowed excitons $e_k h_k$, the oscillator strength at $F=0$ is comparable to the value for bulk GaAs [12]. Given that the electric-dipole matrix elements that matter are all of the same order [19], it follows that $(d\rho/dF)_{F=0} \sim 2ea_0/\Delta \sim 2\mathcal{D}d_{14}/\delta$, i.e., $\rho(e_k h_k) \ll 1$ in the range of interest. Nominally forbidden excitons behave quite differently, for their oscillator strength originates in **q**-dependent mixing of heavy and light holes [12] (**q** is the wave-vector component parallel to the layers). The fact that mixing parameters vary widely among the various branches [12] provides the avenue for enhancement [21]. An illuminating example relevant to our experiments is the case of e_2h_1. Because the h_1 branch does not couple much to l_2 or other branches (l_s indicates light-hole sth-subband states), the oscillator strength of e_2h_1 at $F=0$ is negligible [12]. On the other hand, strong l_1-h_2 hybridization at $\mathbf{q}\neq0$ results in comparable strengths for the ($\mathbf{q}=0$ forbidden) e_2l_1 and the ($\mathbf{q}=0$ allowed) e_2h_2 transitions [12]. As mentioned earlier, the lattice contribution to the electro-optic effect couples h_1 and l_1 (here, coupling to $\Gamma_{7,8}^{c}$ states through the electronic term is not of importance). Thus, if $\gamma\{l_1|h_2\}$ and $\gamma\{l_2|h_1\}$ measure the relevant **q**-induced admixture of the corresponding subbands, $(d\rho/dF)_{F=0} \sim [\gamma\{l_1|h_2\}/\gamma\{l_2|h_1\}]2\mathcal{D}d_{14}/\delta$ and, therefore, $\rho(e_2h_1) \gg \rho(e_kh_k)$ at low fields because $\gamma\{l_1|h_2\} \gg \gamma\{l_2|h_1\}$.

The above considerations are valid in the limit $F \to 0$. Beyond linear respnse, it is convenient to use the following expression:

$$\rho = \frac{F/F_1}{1+(F/F_2)^2} \tag{4}$$

providing a parametrization of the polarization ratio (see later). According to the previous discussion, $F_1 \sim [\gamma\{l_2|h_1\}/\gamma\{l_1|h_2\}]\delta/(2\mathcal{D}d_{14})$ for e_2h_1. Further, since the F dependence of $I_{\parallel}^{+}$ relies mainly on the behavior of the envelope function—like in the quantum-confined Stark effect [1,2]—one obtains the estimate $F_2 \approx \hbar^2/2MeL^3$ where L is the well width and M is the exciton mass. We note that Eq. (4) applies to nominally forbidden transitions. The sign in the denominator reflects the fact that the associated overlap between the electron and the hole envelopes increases with increasing field.

Two QW structures, GaAs-AlAs and GaAs-$\mathrm{Al_{0.35}Ga_{0.65}As}$, grown by molecular-beam epitaxy on (001) n^+-GaAs substrates were used in the experiments. They consist of 40 periods of 90-Å GaAs/40-Å AlAs and 100 periods of 131-Å GaAs/79-Å $\mathrm{Al_{0.35}Ga_{0.65}As}$, respectively. Sample parameters are from growth conditions and measurements of intersubband energies using photocurrent spectroscopy [22]. The sample with AlAs ($\mathrm{Al_{0.35}Ga_{0.65}As}$) barriers was sandwiched between n- and p-type GaAs ($\mathrm{Al_{0.5}Ga_{0.5}As}$) layers doped at $\sim10^{18}$ $\mathrm{cm^{-3}}$ so as to form a p-i-n diode. Devices were processed into mesas of area ~0.2 $\mathrm{mm^2}$ ($\mathrm{Al_{0.35}Ga_{0.65}As}$ barrier QW) and ~0.03 $\mathrm{mm^2}$ (AlAs barrier QW) with Ohmic contacts made by evaporation of Cr/Au and AuGe/Ni. PL measurements were performed at $T=2$ K using various ion and tunable laser sources operating in the range $\lambda_L \approx 650$–710 nm. Not unexpectedly, the polarization behavior of the PL does not depend much on λ_L. Results presented below were obtained with the 676.4-nm $\mathrm{Kr^+}$ line. As with other cases studied, electric-field profiles in our samples exhibit a strong dependence on power density P. In particular, the high-P regime in both structures is that of domains associated with sequential resonant tunneling [22]. In the interest of clarity, the discussion will focus on data at low P (uniform field) for the GaAs-AlAs QW and at high P (domain pattern) for the GaAs-$\mathrm{Al_{0.35}Ga_{0.65}As}$ sample.

Photoluminescence data of the GaAs-AlAs structure showing pronounced anisotropy are reproduced in Fig. 1. In the spectra, the main feature corresponds to e_2h_1 excitons while X results from recombination of AlAs (X) electrons with holes at GaAs (Γ). These assignments are based primarily on calculations of QW energies as a function of electric field. In particular, X exhibits a *blueshift* that is nearly linear in the field and with a slope that is consistent with our assignment (see also [23]). The identification of e_2h_1 is further supported by a combination of photocurrent and PL experiments revealing maxima for the current and the PL intensity at the particular bias for which e_1 and e_2 become aligned (similar results were reported in [24]). Parenthetically, it is worth noticing that the data show an intensity transfer between X and e_2h_1 in the region of crossing which we construe as evidence of their coupling. Such mixing, resembling the well-documented problem of X-e_1h_1 hybridization [23], is possibly the reason why the two excitations have similar polarization properties.

The anisotropy was found to be independent of the po-

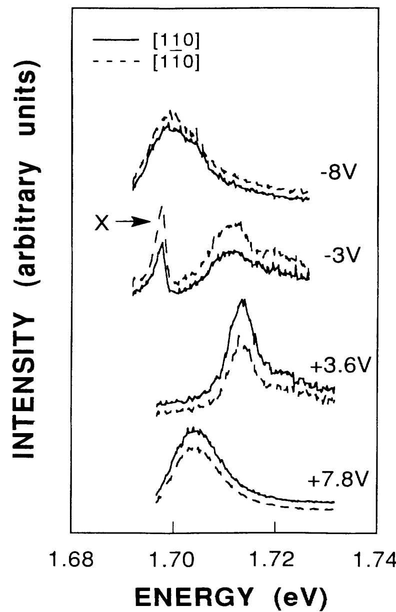

FIG. 1. Polarized PL spectra of the GaAs-AlAs sample showing e_2h_1 recombination at various voltages. Negative values correspond to reverse biases. The peak labeled X is due to barrier → well transitions involving electron AlAs (X) states. The data show large differences between [110] and [1$\bar{1}$0] intensities at low biases. Measurements were performed at $T=2$ K. The excitation wavelength is $\lambda_L=676.4$ nm and the power density is $P=4$ W cm^{-2}.

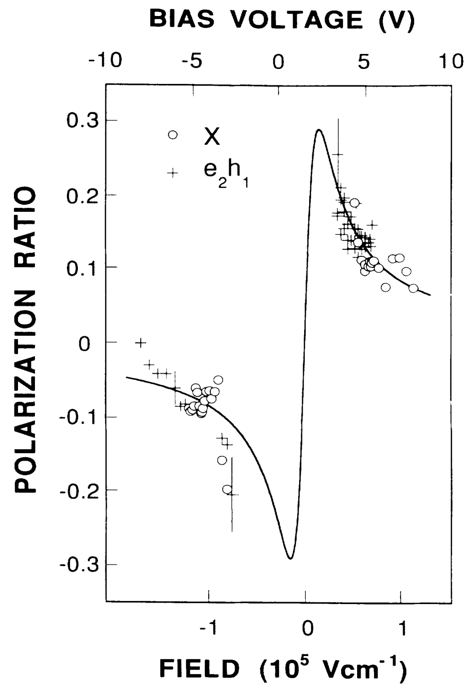

FIG. 2. Polarization ratio $\rho\equiv(\mathcal{I}_{[110]}-\mathcal{I}_{[1\bar{1}0]})/(\mathcal{I}_{[110]}+\mathcal{I}_{[1\bar{1}0]})$ for X and e_2h_1 photoluminescence as a function of the z component of the electric field F and bias V. Here, $F=(V-V_0)/l$ where $V_0\approx 1.5$ V is the built-in voltage and $l\approx 0.57$ μm is the width of the intrinsic region of the device. The solid line is a least-squares fit to the data (see text). Experimental parameters are given in Fig. 1. Results are for the GaAs-AlAs heterostructure.

larization state of the pump and to follow closely the group-theory predictions contained in Eq. (2). Specifically, we find that [110] and [1$\bar{1}$0] are the pair of mutually orthogonal axes exhibiting the largest effect and that these directions exchange their roles after a field reversal. In addition, the comparison between [100]- and [010]-polarized spectra reveals no appreciable differences. Other than e_2h_1 and X, Pockels-like anisotropy was observed for a PL peak due to e_3h_1 (not shown). As already indicated, the dominant e_1h_1 emission at the gap, being 10^3–10^4 times more intense than e_2h_1, is isotropic within experimental error.

Both the strength and the field dependence of the anisotropy support our early treatment of the phenomenon. These characteristics are displayed in the measurements of the polarization ratio [Eq. (3)] as a function of F which are plotted in Fig. 2. Clearly, the large magnitude of the effect and the unusual *decrease* in anisotropy with increasing F are beyond interpretations based solely on bulk properties. However, they can be accounted for by QW effects. The curve in Fig. 2 is a fit by Eq. (4) giving $F_1=2.46\times10^4$ V cm^{-1} and $F_2=1.43\times10^4$ V cm^{-1}. The latter value is consistent with the parameters of our sample while—according to the arguments above—the linear term translates into $\gamma\{l_2|h_1\}/\gamma\{l_1|h_2\}\sim4\times10^{-3}$ which is not unreasonable [12]. Unfortunately, ρ could not be determined for $|F|\lesssim3\times10^4$ V cm^{-1} as the oscillator strength of e_2h_1 becomes negligible. It is in this range where the linear contribution is expected to dominate.

To conclude, we consider as an application high-P results for the GaAs-$Al_{0.35}Ga_{0.65}As$ sample. Anisotropy data for e_2h_1 PL are depicted in Fig. 3. At arbitrary voltages, this structure has been shown to break into electric-field domains characterized by alignment of specific conduction subbands in neighboring wells [22,25]. The inset shows the potential profile for the range inside the arrows. Here, domain e_1-e_2 coexists with the high-field domain resulting from e_1-e_3 alignment. Unlike e_1h_1, e_2h_1 spectra show not a doublet but a single line (its polarization ratio is given in Fig. 3). This reflects the much larger e_2 population of the low-field domain arising from e_1-e_2 resonant tunneling (see [24]). Our measurements complement and are consistent with data obtained using other techniques [22,25]. In particular, ρ is nearly constant in the coexistence region and, as the domain pattern changes, it varies rapidly to signal the disappearance of the domain boundary. The latter phenomenon is poorly understood. Because ρ increases at low fields, our method holds promise for studies of electric fields in a range where standard PL measurements of e_1h_1 energies are not very sensitive [22].

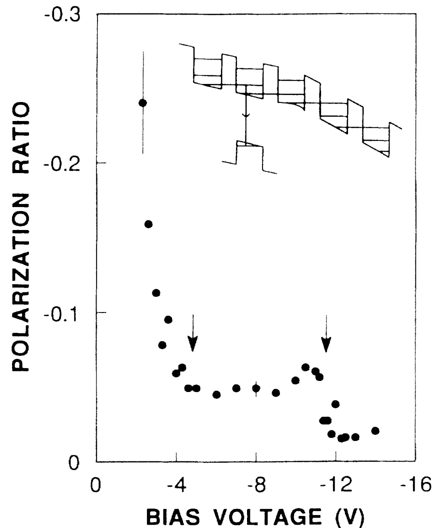

FIG. 3. PL polarization ratio for e_2h_1 in the GaAs-$Al_{0.35}Ga_{0.65}As$ sample at $P=160$ W cm^{-2} ($T=2$ K and $\lambda_L=6764$ Å). Results correspond to the high-P domain regime. Arrows denote biases for which the field is uniform (single domain). The field pattern in the region delimited by the arrows is shown in the inset; PL originates mainly from the low-field domain.

This work was supported by the U.S. Army Research Office (Contract No. DAAL-03-89-K-0047), the University Research Initiative Program (Contract No. AFOSR-90-0214), and the Bunderministerium für Forschung und Technologie of the Federal Republic of Germany. One of us (R.M.) would like to thank M. Cardona for helpful discussions.

[a]Present address: Paul-Drude-Institut für Festkörperelektronik, Hausvogteiplatz 5-7, 0-1086 Berlin, Federal Republic of Germany.

[1] D. A. B. Miller *et al.*, Phys. Rev. B **32**, 1043 (1985), and references therein.
[2] L. Viña *et al.*, Phys. Rev. Lett. **58**, 832 (1987), and references therein.
[3] D. A. B. Miller *et al.*, Appl. Phys. Lett. **45**, 13 (1984).
[4] T. H. Wood *et al.*, IEEE J. Quantum Electron. **21**, 117 (1985).
[5] D. Frölich *et al.*, Phys. Rev. Lett. **59**, 1748 (1987).
[6] J. Bleuse, G. Bastard, and P. Voisin, Phys. Rev. Lett. **60**, 220 (1988).
[7] E. E. Mendez, F. Agulló-Rueda, and J. M. Hong, Phys. Rev. Lett. **60**, 2426 (1988).
[8] P. Voisin *et al.*, Phys. Rev. Lett. **61**, 1639 (1988).
[9] K. W. Goossen, J. E. Cunningham, and W. Y. Jan, Appl. Phys. Lett. **59**, 3622 (1991).
[10] See, e.g., J. B. Krieger and G. I. Iafrate, Phys. Rev. B **33**, 5494 (1986).
[11] Work by B. K. Laurich *et al.*, Phys. Rev. Lett. **62**, 649 (1989), shows that *effective* linear electro-optic coefficients of strained-layer superlattices can be quite large due to piezoelectrically generated fields. This is, however, a secondary effect which (unlike Pockels') does not involve a biaxial indicatrix.
[12] See, e.g., W. T. Masselink *et al.*, Phys. Rev. B **32**, 8027 (1985).
[13] A. Jennings, C. D. W. Wilkinson, and J. S. Roberts, Semicond. Sci. Technol. **7**, 60 (1992).
[14] See, e.g., J. F. Nye, *Physical Properties of Crystals* (Clarendon, Oxford, 1985), Chap. 13.
[15] Comparatively, anisotropies attributable to the Franz-Keldysh effect are rather large at typical fields. See L. V. Keldysh, O. V. Konstantinov, and V. I. Perel, Fiz. Tekh. Poluprovodn. **3**, 1042 (1969) [Sov. Phys. Semicond. **3**, 876 (1970)]. Unlike our case (and Pockels'), the anisotropy in question is uniaxial and field-reversal invariant.
[16] B. H. Kolner and D. M. Bloom, IEEE J. Quantum Electron. **22**, 79 (1986).
[17] C. Y. Fong and Y. R. Shen, Phys. Rev. B **12**, 2325 (1975).
[18] S. Zekeng, B. Prevot, and C. Schwab, Phys. Status Solidi (b) **150**, 65 (1988); I. P. Kaminow and W. D. Johnston, Phys. Rev. **160**, 519 (1967).
[19] See, e.g., M. Cardona, N. E. Christensen, and G. Fasol, Phys. Rev. B **38**, 1806 (1988).
[20] See, e.g., S. Adachi, J. Appl. Phys. **58**, R1 (1985).
[21] Evidently, GaAs QW structures are not the only systems which support a wide range of mixing parameters. In particular, strained-layer heterostructures with strongly modified subbands are promising candidates for enhanced Pockels-like anisotropy. Alternatively, our results can be applied to study mixing in these systems.
[22] See H. T. Grahn, H. Schneider, and K. von Klitzing, Phys. Rev. B **41**, 2890 (1990), and references therein.
[23] M.-H. Meynadier *et al.*, Phys. Rev. Lett. **60**, 1338 (1988).
[24] H. T. Grahn *et al.*, Phys. Rev. Lett. **64**, 2426 (1990).
[25] S. H. Kwok *et al.*, in *Light Scattering in Semiconductor Structures and Superlattices,* edited by D. J. Lockwood and J. F. Young (Plenum, New York, 1991), p. 491.